

Ghost displacement

Gioan Tatsu^a, Ugo Zanforlin^b, Gerald S. Buller^b, and John Jeffers^a

^aDepartment of Physics, University of Strathclyde, John Anderson Building, 107 Rottenrow, Glasgow G4 0NG, UK.

^bInstitute of Photonics and Quantum Sciences, School of Engineering and Physical Sciences, Heriot-Watt University, David Brewster Building, Edinburgh EH14 4AS, UK.

ABSTRACT

We describe a technique whereby a coherent amplitude can be imprinted nonlocally on to a beam of light with thermal statistics that has no phase information on average. We have successfully performed the first experimental realisation. The technique could have applications in the sharing of quantum information and in covert quantum imaging scenarios.

Keywords: quantum optics, quantum imaging, quantum information

1. INTRODUCTION

Ghost imaging is the imaging of objects using light that has not interacted with them. It uses as a resource correlated twin beams that can be produced by either quantum or classical means.¹⁻⁶ It can be performed with correlated twin photons, or simply with classical thermal light. In the latter case the effect exploits the increased degree of second order coherence of thermal light.^{7,8} Both classical and quantum versions are examples of the more general technique of heralding, that allows the probabilistic creation of unusual quantum optical states. Optical heralding typically relies on click-monitoring an optical field mode via a Geiger-mode detector.⁹ When the detector fires it measures the field mode to be not in the vacuum state; it contains at least one photon. In ghost imaging, the detection of light in one beam heralds the other to contain a photon (quantum-correlated twin) or to have a higher mean photon number (classical thermal).¹⁰⁻¹³

The heralding gain G_h of a click-monitored system, the fraction by which the unconditioned mean photon number of the output state \bar{p} is increased on heralding success, is of the order of

$$\begin{aligned} G_h &\sim \frac{\bar{p}+1}{\bar{p}} && \text{quantum,} \\ &\sim 2 && \text{classical.} \end{aligned} \tag{1}$$

The quantum gain can be large for low mean photon number, but this is offset by the fact that the success probability for such a measurement is normally very small, notwithstanding the typically tiny success probability and high resource cost of merely generating the required quantum states. Furthermore, as the mean photon number increases the gain disappears. The classical gain is limited to around 2, but can be applied to a state of any mean photon number. Both ghost imaging and photon “subtraction”^{14,15} experiments with thermal light are typically consistent with this doubling, although the detailed statistics can sometimes be complicated.¹¹

Instead of conditioning on detector-firing events, we can herald the output state differently by effectively comparing the other correlated part of the state with a coherent state by mixing the two at a beam splitter and detecting one output. When the detector does not fire we measure the state to be in a coherent state. This effect has been exploited to amplify coherent states with high gain.¹⁶⁻²⁰ Here we apply this type of technique to a thermal state. The coherent state measurement conditionally reduces the thermal component of the output state and adds a coherent component. This is not the first implementation of useful mixing of coherent light and light with thermal statistics. It has previously been used, in combination with photon subtraction, to implement a probabilistic amplifier.^{21,22} We organise the paper as follows. In Section 2 we provide a brief outline of the theory of the measurement process. Section 3 concerns the experiment and a selection of the results that we obtained. Finally we provide a conclusion and discussion.

Further author information: Send correspondence to J.J. E-mail: john.jeffers@strath.ac.uk

2. THEORY

Suppose that we detect a beam of light using a Geiger-mode detector with perfect quantum efficiency. If the detector does not fire this corresponds to a measurement of the beam in the vacuum state. Conversely, when the detector fires this corresponds to measuring the beam in the complement of the vacuum (Fig. 1 left panel). If the state to be detected in mode 2 undergoes a unitary transformation \hat{U}_2 immediately prior to detection,

Parameters: $\bar{n} = 1$, $r^2 = \frac{2}{3}$

$$d = \frac{t r \bar{n} \alpha}{1 + t^2 \bar{n}} = \frac{\sqrt{2}}{4} \alpha,$$

$$\alpha_{max} = 2.5, \alpha_{min} = 0.5$$

Scale*4 cm

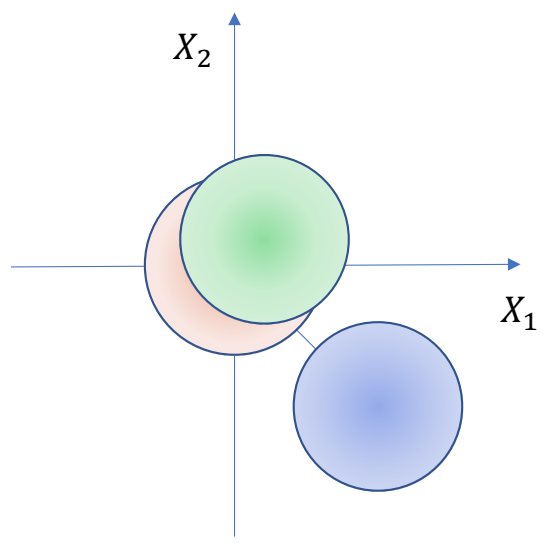


Figure 1. Upper left: Theoretical schematic of the ghost displacement operation. A thermal input state enters mode 1 of a beam splitter, with vacuum input in the mode 2 arm. The transmitted output is displaced and then detected at a Geiger-mode detector. When this detector does not fire the reflected output state is displaced by a coherent amplitude. Lower left: Optical displacement apparatus: The state to be displaced enters a highly-transmitting beam splitter, where it is mixed with a coherent state of amplitude $-\beta/r$. The output state $\hat{\sigma}_{out} = \hat{D}(-\beta)\hat{\sigma}_{in}\hat{D}^{-1}(-\beta)$, where \hat{D} is Glauber's displacement operator, is displaced by amplitude $-\beta$. Right: Quadrature schematic of ghost displacement effects on an input state with $\bar{n} = 1, |r|^2 = 2/3$. Pink obscured uncertainty circle represents unconditioned thermal output state. Green and blue uncertainty circles are ghost displaced outputs with $|\beta| = 0.5$ and $|\beta| = 2.5$ respectively.

Consider next applying this measurement to one of a pair of correlated beams produced by single-mode light with thermal statistics of mean photon number \bar{n} incident on a beam splitter, with vacuum entering the other port, as shown in the left panel of Fig. 1. After unitary mixing the two outputs are in the state

$$\begin{aligned} \hat{\rho}_{12} &= \frac{1}{\pi\bar{n}} \int d^2\alpha e^{-|\alpha|^2/\bar{n}} |\alpha\rangle_1 \langle\alpha| \otimes |0\rangle_2 \langle 0| \\ &\rightarrow \frac{1}{\pi\bar{n}} \int d^2\alpha e^{-|\alpha|^2/\bar{n}} |r\alpha\rangle_1 \langle r\alpha| \otimes |t\alpha\rangle_2 \langle t\alpha|. \end{aligned} \quad (3)$$

If either of the output beams is ignored the state in the other appears thermal, with mean photon number $\bar{n}|r|^2$ or $\bar{n}|t|^2$. There are still two detector outcomes for a nonunit quantum efficiency detector, each of which conditions

the output state. For the no-click outcome, the two-mode state in Eq. (3) becomes an unnormalised reflected one-mode state

$$\begin{aligned}
P_{\times} \hat{\rho}_1^{\text{out}} &= \text{Tr}_2 [\hat{\rho}_{12} \hat{\pi}_{\times}] \\
&= \frac{1}{\pi \bar{n}} \int d^2 \alpha e^{-|\alpha|^2 / \bar{n}} e^{-\eta |\beta - t\alpha|^2} |r\alpha\rangle_1 \langle r\alpha| \\
&= \frac{P_{\times}}{\pi \bar{m}} \int d^2 \alpha e^{-|\alpha - \delta|^2 / \bar{m}} |\alpha\rangle_1 \langle \alpha|,
\end{aligned} \tag{4}$$

where η is the detector quantum efficiency, $\hat{\pi}_{\times} = \sum_n (1 - \eta)^n |n\rangle \langle n|$ is the detection operator corresponding to no clicks and

$$P_{\times} = \frac{e^{-\eta |\beta|^2 / (1 + \eta \bar{n} |t|^2)}}{1 + \eta \bar{n} |t|^2}, \tag{5}$$

$$\bar{m} = \frac{\bar{n} (1 - |t|^2)}{1 + \eta \bar{n} |t|^2}, \tag{6}$$

$$\delta = \frac{\eta \beta \bar{n} t^* (1 - |t|^2)^{1/2}}{1 + \eta \bar{n} |t|^2}. \tag{7}$$

are respectively the probability that the detector does not fire, the output mean thermal photon number and a complex amplitude. The output state produced has the form of a thermal state of mean photon number \bar{m} , indirectly displaced by a coherent amplitude δ – a *ghost displacement* (Fig. 1 right panel). The other possible detection result, when the detector fires, corresponds to conditioning the output arm state with a probability-weighted complement operation.

There are some points to note about the state in Eq. (4). The size of the displacement is *unlimited*; we can choose it and, correspondingly, the mean photon number of the displaced output. Of course, as the magnitude of the displacement becomes larger the success probability of the operation drops (as in Eq. (5)). The main effect of detector quantum efficiency is to reduce the effective displacement size, which we can always offset by increasing β . The output is now also conditionally phase-dependent. We can select its phase by selecting the phase of β .

3. EXPERIMENT

3.1 Set-Up

The experimental schematic is shown in Fig. 2. A vertical cavity surface emitting laser (VCSEL) with a central wavelength of 842.2 nm and a 0.11 nm linewidth, pulsed at a repetition rate of 1 MHz, produced a train of pulses coupled in to a single mode polarization maintaining fiber. A variable optical attenuator (VOA) (not shown) was used to adjust the mean photon number of the pulses to a level compatible with the sensitivity of commercial SPADs. A 90:10 beam splitter routed part of the light to two electro-optic modulators which were used to produce pseudo-thermal light while the remaining unmodulated pulses were sent to the displacement stage. A 50:50 beam splitter (BS₂) was used to split the newly generated thermal light: one output reaching the displacement stage (BS₃) where it was mixed with the pulses corresponding to the displacing coherent state and the other output reaching the tomography stage where a reference signal was chosen to enable full state reconstruction on the ghost-displaced thermal state. The optical set-up comprised two interferometers: one used for the displacement operation and one for state tomography. In order to achieve optimal spatial and temporal overlap between the attenuated laser pulses at the different beam splitters, adjustable air-gaps were inserted in key optical paths, allowing us to adjust and maintain a constant phase reference so that optimal interference visibility could be reached throughout a full integration time. Multiplexed reference signals allowed tuning of each interferometer separately and independently, reaching interferometric visibilities as high as 98%, albeit reducing the effective repetition rate to 250 KHz. The output modes of BS₃ and BS_T were monitored by silicon SPADs (Si-SPADs) with 40% detection efficiency at 850 nm wavelength connected to a time correlation single photon counting (TCSPC) module that collected time tag information for post-processing and correlation analysis with picosecond resolution. The entire set-up was placed in a controlled environment to limit temperature fluctuations and mechanical vibrations.

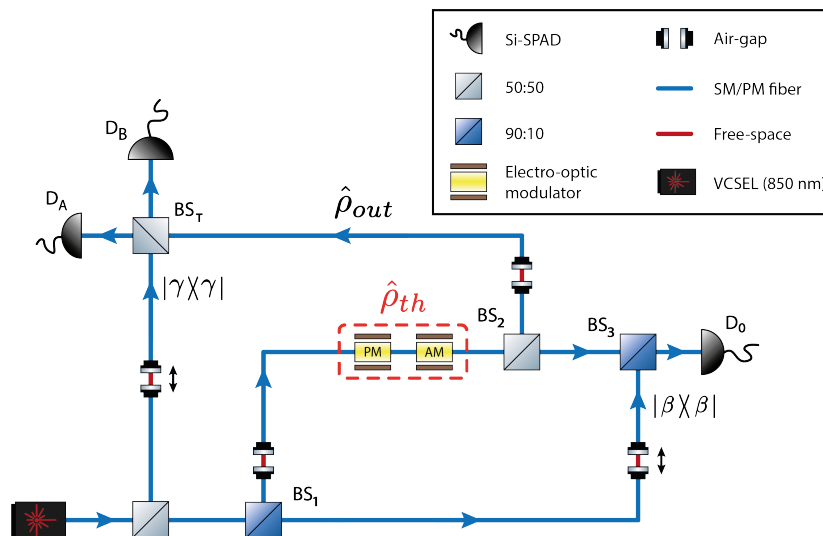


Figure 2. Experimental set-up. A VCSEL source (842.2 nm) produces a train of coherent pulses at 1 MHz repetition rate. Phase and amplitude modulators (PM and AM) modulate individual laser pulses to simulate a pseudo-thermal source. A 90:10 beam splitter (BS_3) performs the displacement operation between the newly generated thermal state and a residual coherent state β that is unmodulated. A “copy” of the thermal state is sent to a tomography stage (BS_T) where a suitable reference signal γ can be chosen to perform a full tomographic reconstruction of the state $\hat{\rho}_{out}$. Phase stabilisation of the interferometers is controlled by adjustable air-gaps. All detectors are Si-SPADs whose signals are registered and processed by a TCSPC module (not shown) for post-processing and correlation analysis.

3.2 Results

Our results show a clear demonstration of the ghost displacement effect. One simple example is in the mean photon number of the conditional output state, which we infer from the count rates at the D_A and D_B detectors. This is shown in Fig. 3 as a function of the displacing amplitude for a mean thermal input photon number of $\bar{n} = 0.5$. There is a clear increase as a function of the displacing amplitude, despite this displacement occurring after the output state has been tapped off. For low displacing amplitudes, the mean photon number is reduced.

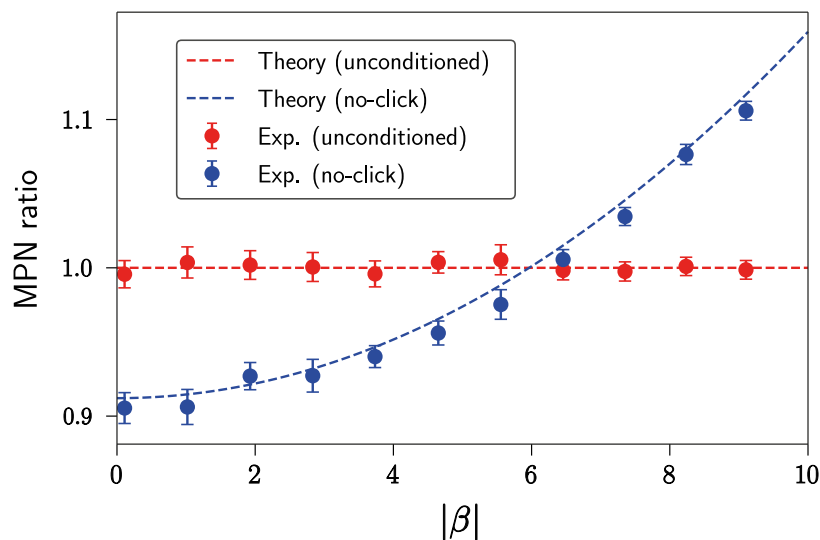


Figure 3. Conditioned mean photon number of the output state (blue dots), relative to the unconditioned mean (red dots), as a function of displacement amplitude, for an input mean photon number of $\bar{n} = 0.5$.

This is in line with our expectations for standard click-based conditioning of thermal light. When $\beta = 0$, we expect a click at the detector to increase the photon number at the output and so when we do not get one, the mean photon number of the output must decrease. As $|\beta|$ increases, the displacement effect kicks in, eventually overcoming the decrease and turning it in to an increase. The fact that none of our displacing amplitude can reach the signal is clearly shown by the independence of the unconditioned line on $|\beta|$.

A more detailed measurement of the individual counts at D_A and D_B shows a significant phase-dependence of the individual count rates after mixing with the reference coherent amplitude γ , which shows that not only has the displaced measurement conditionally increased the mean photon number of the output, but it has also imprinted its phase on the beam nonlocally. The results seen here are repeatable for different thermal mean photon numbers.

4. CONCLUSIONS

We have shown that it is relatively straightforward with current quantum optical technology to displace a thermal state of light in postselection and nonlocally. We have outlined a simple theory of such a ghost displacement and performed the first experiment to verify it. The displaced beam does not interact with any coherent light and so to an outside observer it is indistinguishable from a thermal source. This renders the displacement covert to any outside observer.

The system has several significant advantages over standard conditioning such as used in ghost imaging, based on detectors firing. Firstly, the useful state appears when the detector does not fire, which makes the effect insensitive to poor detector quantum efficiency and to detector dark counts. Secondly, the heralding gain displays the best features of quantum and classical click heralding. It can be high (quantum), effectively unlimited in size and also independent of mean photon number (classical). Furthermore, we get to choose its value by selecting the components of our experiment. This flexibility allows a tailoring of the ghost displaced light to the particular situation required. It also does not require the use of expensive quantum resources, with the consequent stringent limitations on state production probability.

The effects described here are not limited to conditioning measurements based on displacement. We can imagine a scheme that measures in the squeezed vacuum state, which we can accomplish by mixing a squeezed state into the beam splitter in front of the detector in Fig. 1. A no-click at the detector then effectively measures this arm to be in the squeezed vacuum state, with a consequent nonlocal ghost squeezing operation applied to the output state of the device, despite it never coming into contact with a nonlinear optical material.

In summary, thermal light will show large fluctuations in photon number if this property is measured repeatedly by a detector. It also displays complete phase randomness. However, via measurement we have shown that we can imprint lower amplitude and phase fluctuations on the beam, to whatever relative degree that we desire. These properties of the ghost displacement measurement could be exploited in a form of ghost displacement imaging or, for example, in the sharing of phase information covertly at the quantum level.

ACKNOWLEDGMENTS

This work was supported by the UK Engineering and Physical Sciences Research Council (EPSRC) through the Quantum Communications Hub Grant No. EP/T001011/1 and Grant No. EP/N003446/1 and the Quantum Imaging Hub Grant No. EP/T00097X/1. G.T's studentship was funded by the EPSRC Grant No. EP/N509802/1 and the University of Strathclyde.

REFERENCES

- [1] Padgett, M. J. and Boyd, R. W., "An introduction to ghost imaging: quantum and classical," *Phil. Trans. Roy. Soc.* **375**, 20160233 (2017).
- [2] Pittman, T. B., Shih, Y. H., Strekalov, D. V., and Sergienko, A. V., "Optical imaging by means of two-photon quantum entanglement," *Phys. Rev. A* **52**, R3429 (1995).
- [3] Strekalov, D. V., Sergienko, A. V., Klyshko, D. N., and Shih, Y. H., "Observation of two-photon ghost interference and diffraction," *Phys. Rev. Lett.* **74**, 3600–3603 (1995).

- [4] Abouraddy, A. F., Saleh, B. E., Sergienko, A. V., and Teich, M. C., “Role of Entanglement in Two-Photon Imaging,” *Phys. Rev. Lett.* **87**, 123602 (2001).
- [5] Bennink, R. S., Bentley, S. J., and Boyd, R. W., “Two-Photon” Coincidence Imaging with a Classical Source,” *Phys. Rev. Lett.* **89**, 113601 (2002).
- [6] Moreau, P.-A., Toninelli, E., Gregory, T., and Padgett, M. J., “Ghost imaging using optical correlations,” *Laser & Photonics Reviews* **12**(1), 1700143 (2018).
- [7] Loudon, R., “Photon Bunching and Antibunching,” *Physics Bulletin* **27**(1), 21–23 (1976).
- [8] Iskhakov, T., Allevi, A., Kalashnikov, D. A., Sala, V. G., Takeuchi, M., Bondani, M., and Chekhova, M., “Intensity correlations of thermal light,” *The European Physical Journal Special Topics* **199**(1), 127–138 (2011).
- [9] Buller, G. S. and Collins, R. J., “Single-photon generation and detection,” *Journal of Measurement Science and Technology* **21**, 012002 (2010).
- [10] Denis, S., Moreau, P.-A., Devaux, F., and Lantz, E., “Temporal ghost imaging with twin photons,” *Journal of Optics* **19**, 034002 (feb 2017).
- [11] Barnett, S. M., Ferenczi, G., Gilson, C. R., and Speirits, F. C., “Statistics of photon-subtracted and photon-added states,” *Phys. Rev. A* **98**, 013809 (2018).
- [12] Pittman, T., Jacobs, B., and Franson, J., “Heralding single photons from pulsed parametric down-conversion,” *Optics Communications* **246**(4), 545–550 (2005).
- [13] Bogdanov, Y. I., Katamadze, K. G., Avosopiants, G. V., Belinsky, L. V., Bogdanova, N. A., Kalinkin, A. A., and Kulik, S. P., “Multiphoton subtracted thermal states: Description, preparation, and reconstruction,” *Phys. Rev. A* **96**, 063803 (Dec 2017).
- [14] Parigi, V., Zavatta, A., Kim, M., and Bellini, M., “Probing quantum commutation rules by addition and subtraction of single photons to/from a light field,” *Science* **317**, 1890–1893 (2007).
- [15] Allevi, A., Andreoni, A., Bondani, M., Genoni, M. G., and Olivares, S., “Reliable source of conditional states from single-mode pulsed thermal fields by multiple-photon subtraction,” *Phys. Rev. A* **82**, 013816 (2010).
- [16] Eleftheriadou, E., Barnett, S. M., and Jeffers, J., “Quantum Optical State Comparison Amplifier,” *Phys. Rev. Lett.* **111**, 213601 (2013).
- [17] Donaldson, R. J., Collins, R. J., Eleftheriadou, E., Barnett, S. M., Jeffers, J., and Buller, G. S., “Experimental Implementation of a Quantum Optical State Comparison Amplifier,” *Phys. Rev. Lett.* **114**, 120505 (2015).
- [18] Donaldson, R. J., Mazzarella, L., Zanforlin, U., Collins, R. J., Jeffers, J., and Buller, G. S., “Quantum state correction using a measurement-based feedforward mechanism,” *Phys. Rev. A* **100**, 023840 (2019).
- [19] Donaldson, R., Mazzarella, L., Collins, R., Jeffers, J., and Buller, G., “A high-gain and high-fidelity coherent state comparison amplifier,” *Communications Physics* **1**, 54 (2018).
- [20] Canning, D. W., Donaldson, R. J., Mukherjee, S., Collins, R. J., Mazzarella, L., Zanforlin, U., Jeffers, J., Thomson, R. R., and Buller, G. S., “On-chip implementation of the probabilistic quantum optical state comparison amplifier,” *Optics Express* **27**, 31713–31726 (2019).
- [21] Marek, P. and Filip, R., “Coherent-state phase concentration by quantum probabilistic amplification,” *Phys. Rev. A* **81**, 22302 (2010).
- [22] Usuga, M. A., Müller, C. R., Wittmann, C., Marek, P., Filip, R., Marquardt, C., Leuchs, G., and Andersen, U. L., “Noise-powered probabilistic concentration of phase information,” *Nature Physics* **6**(10), 767–771 (2010).